Indium $\sqrt{7} \times \sqrt{3}$ on Si(111): A Nearly Free Electron Metal in Two Dimensions

Eli Rotenberg,[1] H. Koh,[1] K. Rossnagel,[1] H.W. Yeom,[2] J. Schäfer,[3] B. Krenzer,[4] M. P. Rocha,[4] and S. D. Kevan[4]

[1]*MS 6-2100, Advanced Light Source, Lawrence Berkeley National Laboratory, Berkeley, California 94720, USA*
[2]*Institute of Physics and Applied Physics, Yonsei University, 134 Sinchon-dong, Seodaemun-gu, Seoul 120-749, Korea*
[3]*Institute of Physics, University of Augsburg, Universitätsstraße 1, D-86159 Augsburg, Germany*
[4]*Department of Physics, University of Oregon, Eugene, Oregon 97403, USA*

(Received 8 August 2003; published 11 December 2003)

We present measurements of the Fermi surface and underlying band structure of a single layer of indium on Si(111) with $\sqrt{7} \times \sqrt{3}$ periodicity. Electrons from both indium valence electrons and silicon dangling bonds contribute to a nearly free, two-dimensional metal on a pseudo-4-fold lattice, which is almost completely decoupled at the Fermi level from the underlying hexagonal silicon lattice. The mean free path inferred from our data is quite long, suggesting the system might be a suitable model for studying the ground state of two-dimensional metals.

DOI: 10.1103/PhysRevLett.91.246404 PACS numbers: 71.18.+y, 73.20.At, 73.50.–h, 79.60.–i

Because of enhanced many-body interactions, quasi-two-dimensional (2D) electron systems present diverse electronic phenomena such as charge density waves [1], metal-insulator transitions [2–4], Wigner lattices [5], and high-temperature superconductivity [6]. Metal monolayers on semiconductors might be attractive to study such phenomena, not only because their electronic states could be probed directly by surface-sensitive means, but also because their electrons could be confined to a single monolayer thickness. As such, they might approach an ideal two-dimensional limit, as opposed to quasi-2D systems such as layered compounds in which there remains significant interlayer coupling [7].

In this Letter, we report angle-resolved photoemission spectroscopy measurements of a model system, $\sqrt{7} \times \sqrt{3}$ indium on Si(111), which displays a high degree of localization to the 2D layer and whose Fermi surface is strikingly close to the ideal 2D electron gas (2DEG). We show that the metallic layer's cohesion is so strong that nearly all the electrons available (indium valence + silicon dangling bonds) participate in the 2DEG with only a minority participating in covalent In-Si bonds. As a consequence of the confinement to the 2D layer, the potential felt by the electrons has nearly the pseudo-4-fold symmetry of the bare, isolated overlayer, with only minor effects arising from the hexagonal substrate symmetry. The mean free path for electron scattering at the Fermi level is quite long, suggesting that this system may be suitable for future investigations of the ground state properties of 2D metals.

A Si(111) crystal, miscut 2° towards $[11\bar{2}]$, was heated by direct current to obtain a 7×7 reconstruction. After depositing >1.5 ML (monolayer) In and annealing to 500–600 K to remove the excess In, we observed the $\sqrt{7} \times \sqrt{3}$ low energy electron diffraction (LEED) pattern shown in Fig. 1(a). Although three equivalent 120° rotated domains are possible, with careful annealing treatment, probably assisted by substrate step ordering, we reproducibly obtained the single-domain pattern shown in Fig. 1(a). The strongest recurring spots are those indicated by the large circles (inset), although the remaining $\sqrt{7} \times \sqrt{3}$ spots (small circles) can also be observed depending on the electron energy. Although Kraft *et al.* [8,9] reported the coexistence of 1.2 ML pseudo-4-fold (PFF) and 1.0 ML pseudo-6-fold phases, our x-ray photoelectron diffraction measurements [10] support a pure PFF phase. Apparently, our preparation method kinetically favors the 4-fold over the 6-fold phase.

After preparation, the samples were transferred *in vacuo* to a He-cooled goniometer capable of sample rotations along two orthogonal polar axes plus azimuth. Angle-resolved photoemission was performed with a

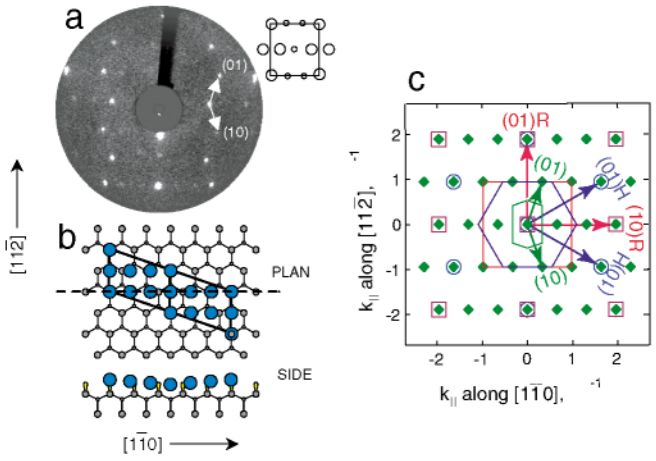

FIG. 1 (color online). Structural characterization of $\sqrt{7} \times \sqrt{3}$ indium on Si(111). (a) LEED pattern at 144 eV. The inset indicates the strongest spots relative to the $\sqrt{7} \times \sqrt{3}$ Brillouin zone. (b) Plan view of the $\sqrt{7} \times \sqrt{3}$ unit cell of indium atoms determined by Kraft *et al.* [8,9]. (c) The reciprocal lattice points **G**, the basis vectors $[(hk)H$, $(hk)R$, and $(hk)]$ and Brillouin zones for unreconstructed 1×1, rectangular pseudo-4-fold, and $\sqrt{7} \times \sqrt{3}$ symmetries, respectively.

hemispherical analyzer (Gammadata SES100) at beam line 7.0 of the Advanced Light Source. The total energy resolution (photons + electrons) was about 50 meV. The conversion from emission angle to two-dimensional momentum is accomplished through a simple trigonometric transformation. The photon polarization was linear and lay in the scattering plane, roughly parallel to $[1\bar{1}0]$. Samples were measured at 30–40 K.

Figure 1(b) shows the PFF structure of the overlayer proposed by Kraft *et al.* [8,9]. It is notable that the rectangular overlayer symmetry differs so much from the hexagonal substrate. Although the overlayer is commensurate with the substrate over a large $\sqrt{7} \times \sqrt{3}$ unit cell, the overlayer-substrate arrangement appears locally incommensurate. Therefore, it is useful to consider the corresponding reciprocal-space Brillouin zone (BZ) as well as reciprocal lattice vectors **G** and basis vectors for three relevant symmetries found in this system [Fig. 1(c)]: the fundamental $\sqrt{7} \times \sqrt{3}$ lattice, the bulk-terminated Si hexagonal lattice, and the reduced, rectangular PFF unit cell obtained if all In atoms were identical. These **G** vectors are denoted by (hk), $(hk)H$, and $(hk)R$, respectively.

Figure 2(a) shows a momentum map of the photoemission intensity from a narrow (≈ 150 meV) energy window centered on E_F. We find a striking array of nearly circular Fermi contours; the strongest of these represent a simple 2D metal on a nearly square lattice, which is discussed in many elementary solid state treatments. The raw data, taken over the quadrant $(k_x, k_y) > -0.5$ Å^{-1}, were mirror symmetrized across these axes (although not strictly a mirror plane, we observed approximate mirror symmetry across the k_x axis).

To model the observed Fermi surface, we used a simple plane wave pseudopotential model in which the potential is projected onto reciprocal space as $V(\mathbf{r}) = \sum_{\mathbf{G}} V_{\mathbf{G}} e^{i\mathbf{G}\cdot\mathbf{r}}$ such that nearly free electron bands with dispersion

$$E = (\hbar^2/2)(k_x^2/m_x^* + k_y^2/m_y^*) \qquad (1)$$

are found centered on each possible **G** vector of the reciprocal lattice. Thirty-nine **G** vectors (some equivalent by symmetry) were sufficient to account for practically all the features in the experimental intensity map. This calculation together with the data are shown in Fig. 2(b), in which the experimental data has been appropriately symmetrized (translation + reflection) into the reduced $\sqrt{7} \times \sqrt{3}$ Brillouin zone.

Choosing the effective masses $m_{x,y}^* = (1.1e, 1.08e)$ and the Fermi energy (6.9 eV) brings the data and model into excellent agreement along the broad circular arcs. Only one principle pseudopotential coefficient (discussed further below) is needed to account for the anticrossing gap labeled *a* in Fig. 2(b). Conversely, the model and data differ significantly at the central "butterfly" feature in two ways. The first is that the experimental butterfly

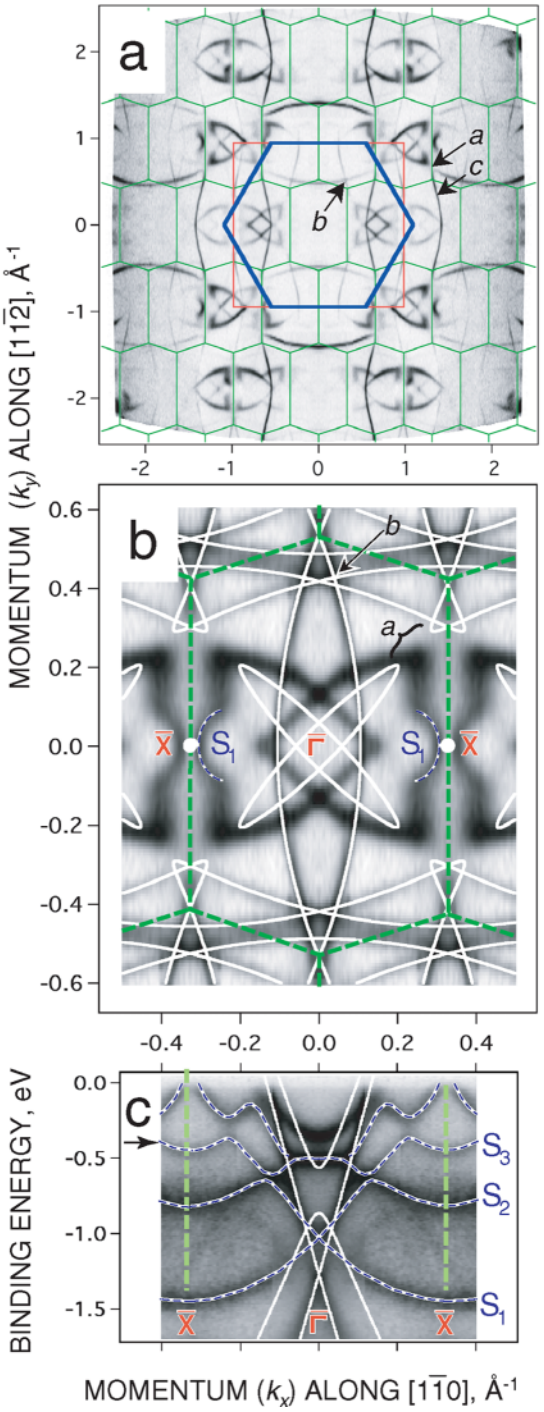

FIG. 2 (color online). Fermi contours and underlying bands of $\sqrt{7} \times \sqrt{3}$ indium on Si(111). (a) The intensity at E_F for $h\nu = 89.5$ eV, together with Brillouin zones from Fig. 1. Raw data are shown in the upper right quadrant. The rest of the data are obtained by mirror symmetry operations. (b) The experimental data of (a) averaged over each $\sqrt{7} \times \sqrt{3}$ Brillouin zone according to translational/reflection symmetry, together with a plane-wave calculation for $\sqrt{7} \times \sqrt{3}$ symmetry as described in the text. (c) The measured electronic bands similarly backfolded in the reduced BZ for the line $k_y = 0$. The overplotted bands are solid (simulated) and dashed (guides to the eye). The top of the bulk silicon valence band maximum is indicated by an arrow.

"wings" are much larger than that of the model, leading the predicted position of gap a to differ from the experiment. A second, more important difference is the presence of two elliptical protrusions S_1 not predicted by the simple model, which we will return to later.

We now consider the nature of the In-Si chemical bond and its influence on the Fermi surface topology. In the PFF unit cell there is one In atom (of valence 3) and 5/6 unsaturated Si atoms (contributing one electron each) for a total of 3.833 electrons. We find the central circular contour [c in Fig. 2(a)] to cover 1.725 times the PFF BZ, or 3.45 electrons per indium atom, far in excess of the three available indium valence electrons. Although some additional charge might come from bulk electrons trapped at the surface by a band-bending potential [11], the charge density associated with such accumulation layers is far too small (typically $10^{11}e/\mathrm{cm}^2$) to account for the excess charge.

We conclude that the 2D metal has contributions not only from the In atoms but also from about half of the surface silicon dangling bonds. This is not unreasonable considering the structural model in Fig. 1(b). The diversity of In-Si arrangements suggests the possibility of multiple types of In-Si bonds. Each interfacial Si atom contributes a single protruding dangling bond electron, some of which bond covalently with overlying indium atoms, and some of which may protrude into their interstices. We speculate that these interstitial dangling bonds are donated to the charged layer, increasing the electron count from 3 to 3.45 electrons per indium atom. This is a very surprising kind of bond, much more characteristic of metallic bonding than the directional covalent bonding expected of semiconductors. The large gain in cohesive energy by this charge donation to the In layer must offset the large energy loss associated with vacating the dangling bond, thus providing evidence that the dominant interaction determining the structure is metallic In-In and not covalent In-Si bonding [8,9].

The remaining dangling bonds participate in a more conventional In-Si covalent bond. This appears to be the origin of the extra S_1 features in Fig. 2(b), which cannot be accounted for by our simple nearly free electron model (white lines). In contrast to these minor alterations to the Fermi contours, the underlying band structure [Fig. 2(c)] is quite surprising: a set of three parabolic bands (S_{1-3}) are observed; not only mixing with each other, these states apparently mix with the free electron bands near $\overline{\Gamma}$, effectively raising the effective mass of these states there. This therefore accounts for the enlargement of the butterfly wings centered on $\overline{\Gamma}$ compared to our model.

How many electrons are represented by S_{1-3}? Considering the wide range of these states along $[1\bar{1}0]$ [see Fig. 2(c)] and along $[11\bar{2}]$ (about 20% of the $\sqrt{7}\times\sqrt{3}$ BZ), we can conservatively estimate at least 0.3 electrons per indium atom. Together with the 0.45 electrons donated directly to the free electron bands, we have more or less accounted for the $5/6 = 0.833$ electrons expected from Si dangling bonds.

If the electrons are mostly confined to the In layer, then they should "feel" the PFF symmetry more than the hexagonal symmetry of the substrate. In our model we find a circular Fermi contour centered on each $V_{\mathbf{G}}$. Since the observed photoemission intensity for a circle centered at $\mathbf{G}$ goes as the square of the corresponding $V_{\mathbf{G}}$ [12], then by inspection of Fig. 2(a), we can rank the potential at $\mathbf{G} = (11)R$ as the most important followed by $\mathbf{G} = (01)R$, $(10)R$, $(01)H$, and then all the others. Although additional circles are found centered on practically all the other, higher symmetry $\sqrt{7}\times\sqrt{3}$ $\mathbf{G}$s, they are much weaker and observable only in unconnected sections of arc. This shows that the pseudopotentials associated with the rectangular In lattice greatly dominate the potential.

Quantitative estimates of $V_{\mathbf{G}}$ in this fashion are difficult since the photoemission intensities are subject to strong systematic energy-dependent intensity deviations (similar to those in the LEED patterns [13,14]). Absolute measurements of $V_{\mathbf{G}}$ are possible because of the mixing of bands whose centers are connected by $\mathbf{G}$. This mixing results in anticrossing gaps in energy and momentum [e.g., gap a in Figs. 2(a) and 2(b)]. In order to reproduce this gap we used a value $V_{(11)R} = 0.15$ eV for our simulation. Apart from this anticrossing gap a, there is no experimentally resolved gap at E_{F} for any other potential terms $V_{\mathbf{G}}$, which must all therefore be less than about 25 meV.

At deeper binding energies, on the other hand, we found gaps at several other crossings; for example, the potential term $V_{(01)H}$ [affecting the b intersection in Fig. 2(a)] was found to induce a gap for binding energies greater than 0.8 eV. This makes sense because, as the bands come into resonance with the underlying bulk Si bands, their wave functions penetrate deeper towards the substrate and therefore the potential terms associated with the hexagonal silicon lattice become more important.

Some authors [14,15] have described the presence of such weak replica bands as we see in Fig. 2 as due not to weak potentials $V_{\mathbf{G}}$ felt by the electron in the initial state, but rather as a consequence of final state surface umklapp scattering from the corresponding surface $\mathbf{G}$ vectors. To the extent that this occurs, it would strengthen our claim that the potential contribution of the substrate symmetry on the initial state is negligible. Normally, surface umklapp scattering is ascribed as the third step in a three step model for photoemission from bulk bands (excitation, transport to the surface, scattering by the surface potential). We conservatively assign the replica bands to initial-state potential effects; however, in the absence of anticrossing gaps for the weak replica bands, it remains difficult to eliminate final state scattering as their cause.

The remarkable sharpness of the bands attests to the high quality of the films and long mean free path (MFP)

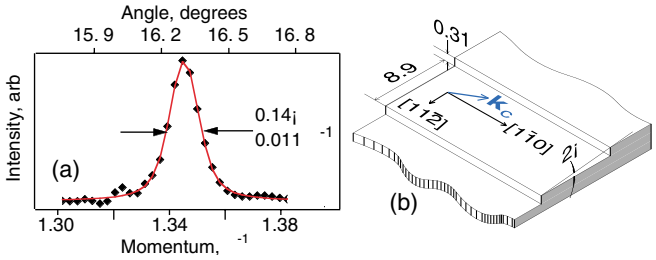

FIG. 3 (color online). (a) Momentum distribution curve at E_F for point c of Fig. 2. (b) Average terrace geometry (dimensions in nanometers). The crossing corresponds to the momentum vector $\mathbf{k}_c$.

of the carriers. The latter is enhanced by the large energy difference (0.4 eV) between E_F and the silicon valence band maximum [arrow in Fig. 2(c)]. Since E_F is pinned near midgap, this surface represents nearly the best localization of electrons to the surface layer which can be achieved on Si.

To estimate the MFP, we measured the momentum distribution along $\mathbf{k}_c$ (point c of Fig. 2) and fitted the data to a Gaussian-broadened Lorentzian (Fig. 3). The Gaussian broadening was fixed to 0.11° (0.0086 Å^{-1}), which is a lower limit given by our detector geometry and energy resolution. The Lorentzian width $\delta k \lesssim 0.0067$ Å^{-1} gives a MFP of $1/\delta k \gtrsim 150$ Å [16]. This MFP is comparable with the average terrace width (~430 Å) projected along $\mathbf{k}_c$ [see Fig. 3(b)]. So while the measured lifetime is already quite long for as-deposited 2D metals, we believe that the lifetime is at least partially determined by scattering at the step edges and, in fact, the MFP within the terraces is significantly longer than 150 Å.

Currently the zero-field ground state of two-dimensional electron gases is controversial, as is the relative roles of disorder, pairing interactions, and electron-electron correlation[4]. Considering the high electron density (3.6×10^{15} cm^{-2}), electron-electron interactions should be screened out and in the inevitable presence of defects the ground state should be insulating [17,18]. On the other hand, pairing is still important: our temperature-dependent valence band linewidths [19] (not shown) indicate an electron-phonon coupling constant $\lambda \simeq 1$, similar to that of bulk indium. We might therefore expect the surface to become superconducting near the critical temperature of bulk In ($T_c = 3.4$ K). We propose that temperature-dependent measurements as a function of defect density (controlled by adsorbate deposition) may clarify the zero-field two-dimensional ground state.

In summary, extensive high-resolution band structure measurements, supported by simulations, show that the electronic structure of $\sqrt{7} \times \sqrt{3}$ In/Si(111) consists of two manifolds of bands. Most electrons are found in a nearly-free electron metallic band on a pseudo-4-fold lattice potential, with a minority of electrons in a second set of bands ascribed to covalent In-Si bonds. Coupling between the dominant free electron gas and the remaining interface states is confined to a relatively small part of the Fermi surface near $\bar{\Gamma}$ where the bulk valence band edge comes closest to the Fermi level. The mean free path inferred from our data is at least partially limited by the scattering at step edges, reflecting the very high quality of films grown. These films may be suitable for studying ground state properties of low-dimensional metals.

This work was supported by the U.S. DOE under Grants No. DE-FG06-86ER45275 and No. W-7405-Eng-48. The ALS is operated under Contract No. DE-AC03-76SF00098 at Lawrence Berkeley National Laboratory. H. W. Y. is supported by KOSEF through ASSRC and by MOST through CAWL of the CRi program.

[1] G. Grüner, *Density Waves in Solids* (Addison-Wesley, Reading, MA, 1994).
[2] P. W. Anderson, Phys. Rev. **109**, 1492 (1958).
[3] S. V. Kravchenko, G. V. Kravchenko, J. E. Furneaux, V. M. Pudalov, and M. D'Iorio, Phys. Rev. B **50**, 8039 (1994).
[4] M. S. E. Abrahams and S. Kravchenko, Rev. Mod. Phys. **73**, 251 (2001).
[5] E. P. Wigner, Phys. Rev. **46**, 1002 (1934).
[6] G. Bednorz and K. A. Müller, Z. Phys. B: Condens. Matter **64**, 189 (1986).
[7] K. Rossnagel, L. Kipp, M. Skibowski, C. Solterbeck, T. Strasser, W. Schattke, D. Voß, P. Krüger, A. Mazur, and J. Pollmann, Phys. Rev. B **63**, 125104 (2001).
[8] J. Kraft, S. L. Surnev, and F. P. Netzer, Surf. Sci. **340**, 36 (1995).
[9] J. Kraft, M. G. Ramsey, and F. P. Netzer, Surf. Sci. **372**, L271 (1997).
[10] E. Rotenberg *et al.*, Mater. Res. Soc. Symp. Proc. **648**, 10 (2001).
[11] D. C. Tsui, Phys. Rev. Lett. **24**, 303 (1970).
[12] E. Rotenberg, W. Theis, and K. Horn, J. Alloys Compd. **342**, 348 (2002).
[13] R. Losio, K. N. Altmann, and F. J. Himpsel, Phys. Rev. B **61**, 10 845 (2000).
[14] H. J. Neff, I. Matsuda, M. Hengsberger, F. Baumberger, T. Greber, and J. Osterwalder, Phys. Rev. B **64**, 235415 (2001).
[15] J. N. Crain, K. N. Altmann, C. Bromberger, and F. J. Himpsel, Phys. Rev. B **66**, 205302 (2002).
[16] D. Y. Petrovykh, K. N. Altmann, H. Höchst, M. Laubscher, S. Maat, and G. J. Mankey, Appl. Phys. Lett. **73**, 3459 (1998).
[17] E. Abrahams, P. W. Anderson, D. C. Licciardello, and T. V. Ramakrishnan, Phys. Rev. Lett. **42**, 673 (1979).
[18] A. R. Hamilton, M. Y. Simmons, M. Pepper, E. H. Linfield, P. D. Rose, and D. A. Ritchie, Phys. Rev. Lett. **82**, 1542 (1999).
[19] T. Balasubramanian, E. Jensen, X. L. Wu, and S. L. Hulbert, Phys. Rev. B **57**, 6866 (1998).